Optical Control of Excitons in a Pair of Quantum Dots Coupled by the Dipole-Dipole Interaction

Thomas Unold,[1] Kerstin Mueller,[1] Christoph Lienau,[1,*] Thomas Elsaesser,[1] and Andreas D. Wieck[2]

[1]*Max-Born-Institut für Nichtlineare Optik und Kurzzeitspektroskopie, D-12489 Berlin, Germany*
[2]*Lehrstuhl für Angewandte Festkörperphysik, Ruhr-Universität, 44870 Bochum, Germany*
(Received 5 October 2004; published 8 April 2005)

We demonstrate coherent nonlinear-optical control of excitons in a pair of quantum dots (QDs) coupled via dipolar interaction. The single-exciton population in the first QD is controlled by resonant picosecond excitation, giving rise to Rabi oscillations. As a result, the exciton transition in the second QD is spectrally shifted and concomitant Rabi oscillations are observed. We identify coupling between permanent excitonic dipole moments as the dominant interaction mechanism, whereas quasiresonant (Förster) energy transfer is weak. Such control schemes based on dipolar interaction are a prerequisite for realizing scalable quantum logic gates.

Dipole-dipole coupling represents an elementary interaction in nature, playing a key role for structure and function of many atomic, (macro)molecular, and solid-state systems. Examples are, e.g., light harvesting in bacterial photosynthetic units [1,2], excitation transport in molecular aggregates or polymers [3], or vibrational energy transfer in water [4]. Recently, dipole-dipole interaction schemes have also been proposed for implementing novel quantum function in man-made nanostructures such as semiconductor quantum dots [5,6]. There is a very wide range of dipole-dipole interaction strengths, depending on the spatial arrangement, i.e., orientation and separation of dipoles, and the microscopic interaction mechanism, such as permanent dipole couplings, van der Waals dispersion forces, or Förster dipole energy transfer. A well-defined geometry of the interacting dipoles on a (sub)nanometer length scale is required to analyze the coupling mechanisms in a quantitative way. Thus, studies of single nanosystems and/or ordered nanoarrays [7] are particularly desirable. First experiments have investigated a pair of molecules in an organic crystal [8] or the light-harvesting-2 complex [9] and have been performed with steady-state techniques. Here, we demonstrate that combining high spatial resolution with time-resolving optical techniques allows for a separation of different couplings through their individual real-time dynamics and for controlling nanosystems on ultrashort time scales.

We study dipolar couplings between two individual semiconductor quantum dots. Coherent manipulation of the exciton state of a single QD is evidenced by probing Rabi oscillations. We demonstrate how this single exciton interacts with a second QD in its neighborhood and analyze the coupling mechanism. As a model system we use interface quantum dots (QD) formed in thickness fluctuations of a 5.1 nm (100) GaAs quantum well (QW) grown by molecular beam epitaxy between two AlAs/GaAs superlattice barriers on a (100) GaAs substrate and buried 120 nm below the surface [10]. The optical properties of these QDs are governed by exciton localization in confinement potentials of typically 10 meV. These QDs show narrow, atomiclike photoluminescence (PL) lines and excitation spectra [11], and dephasing times of 30–50 ps [12]. Despite these short decoherence times, most of the DiVincenzo criteria [13] for quantum computation have been demonstrated on this class of QDs, specifically single qubit rotations [14], electrical and ultrafast optical readout [14–16], and a two-qubit gate operation in a single QD [17]. So far, however, little is known about electronic couplings between individual QDs, required for implementing scalable quantum gates.

Time-dependent nonlinear spectra are recorded at a temperature of 12 K using a near-field optical microscope with a spatial, temporal, and spectral resolution of 200 nm, up to 200 fs, and $100\,\mu$eV, respectively [15,18]. Spectrally tunable 2-ps pump pulses with a bandwidth of $\sigma = 0.8$ meV and weak, spectrally much broader ($\sigma = 10$ meV) probe pulses are both coupled into an etched, uncoated near-field tip. The reflected probe light is collected through the same tip, spectrally dispersed, and recorded with a charge coupled device (CCD) camera (Fig. 1). We measure the pump-laser induced change in the reflected probe laser spectrum $\Delta R(\omega, \Delta t) = [R(\omega, \Delta t) - R_0(\omega)]$ at a fixed spatial tip position as a function of the time delay Δt between pump and probe pulses [15]. R_0 denotes the reflected probe laser spectrum in the absence of the pump.

The relevant excitonic transitions in an isolated QD can be represented by an effective four-level system, consisting of the crystal ground state $|00\rangle$, two nearly degenerate single-exciton states with orthogonal polarization orientation, $|10\rangle$ and $|01\rangle$, and the biexciton state $|11\rangle$. Population control of state $|10\rangle$ is achieved by resonant impulsive excitation with a linearly polarized light pulse much shorter than the decoherence time T_2 of the $|00\rangle \rightarrow |10\rangle$ transition. In this case, the $|10\rangle$ population after the interaction with the excitation laser is given as $n_{10} = \sin^2(\theta/2)$, with the pulse area $\theta = [(\vec{\mu} \cdot \vec{\varepsilon})/\hbar] \int_{-\infty}^{\infty} E_p(t)dt$ [16,17]. An increase of the driving electric field and, thus, θ, leads
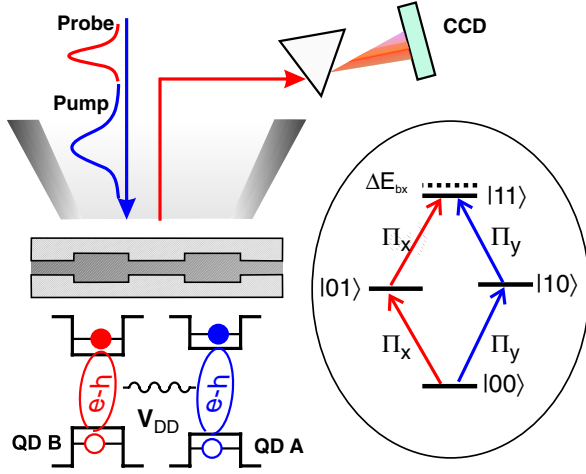
FIG. 1 (color online).   Schematic of the experiment: two optical pulses are coupled into a near-field probe to study the nonlinear response of two semiconductor quantum dots coupled by dipole-dipole interaction V_{DD}. Inset: schematic energy diagram of one QD and optical polarization selection rules.

to population oscillations. Such Rabi oscillations have been observed only recently for single semiconductor QDs [14,16,17].

Experimentally, we select single QDs with the near-field tip as confirmed by PL and ΔR spectra recorded for non-resonant excitation at a fixed spatial position [Fig. 2(a)]. Resonant excitation at the $|00\rangle \rightarrow |10\rangle$ transition causes a new transition to appear at 1.648 eV in the ΔR spectrum [Fig. 2(b)]. Its absorptive line shape and positive sign allow to assign it to the exciton-biexciton $|10\rangle \rightarrow |11\rangle$ transition of QD A. The integrated area of the biexciton line $\Delta R_{XX} =$
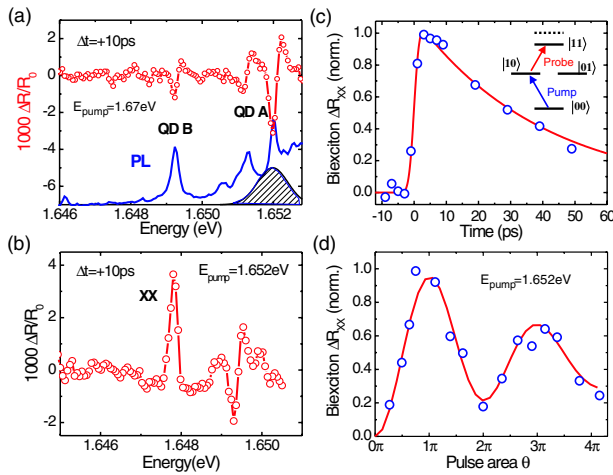
$\int \Delta R d\omega$ monitors the population of state $|10\rangle$. The temporal dynamics of $\Delta R_{XX}(\Delta t)$ [Fig. 2(c)] shows a resolution-limited rise and an exponential decay on a 40 ps time scale, the single-exciton population lifetime $T_{1,A}$. When varying the excitation strength, $\Delta R_{XX}(\Delta t = 10$ ps$)$ displays pronounced oscillations, evidence for Rabi oscillations on the $|00\rangle \rightarrow |10\rangle$ transition [Fig. 2(d)]. The amplitude of this oscillation decreases with increasing θ, a behavior most likely due to excitation-induced dephasing: the pump pulse not only drives the exciton transition in QD A but also creates optical excitations in the environment of the QD. Because of their Coulomb interactions with the QD dipole, such excitations give rise to fluctuations of the QD resonance energy and, thus, to decoherence [15] of the QD polarization. The results are quite well reproduced within a phenomenological optical Bloch equation model by assuming an interband dipole moment of 60 D and an intensity-dependent dephasing rate $\gamma = 1/T_2 + \gamma_1 E_{pu}^2$, neglecting other possible mechanisms causing a damping of the Rabi oscillations. The modeling indicates that the dephasing rate increases from less than $(15$ ps$)^{-1}$ (given by the finite monochromator resolution) to about $(6$ ps$)^{-1}$ for $\theta = 3\pi$.

To probe dipole interactions between two individual QDs, we now study the effect of a single-exciton excitation of QD A on the optical nonlinearity of a neighboring QD B probed simultaneously in Fig. 2(a). In Fig. 3(a), we display nonlinear spectra ΔR_B of QD B recorded with resonant excitation of QD A. The excitation conditions are identical to those in Fig. 2(c) with an excitation pulse area of $\theta = 0.75\pi$.
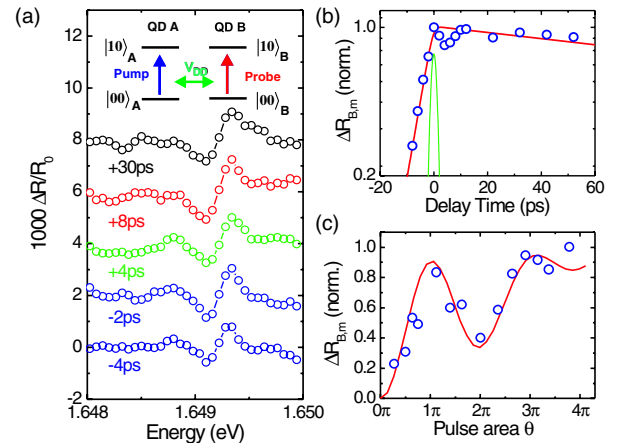

FIG. 2 (color online).   (a) Population control of single excitons. Near-field PL and ΔR spectra for excitation above the QW band gap. (b) Pump-induced biexciton nonlinearity at 1.648 eV. The pump laser [shaded area in (a)] is tuned to QD A and $\Delta t = 10$ ps. (c) Time dynamics of ΔR_{XX}. (d) Rabi oscillation in a single QD. Magnitude of $\Delta R_{XX}(\Delta t = 10$ ps$)$ as a function of the pulse area θ of the pump laser. The solid lines in (c) and (d) show optical Bloch equation simulations.

FIG. 3 (color online).   (a) Nonlinear ΔR spectra of quantum dot B for resonant single-exciton excitation of QD A at 1.652 eV as a function of time delay Δt. The pulse area of the 2-ps excitation pulses is $\theta \simeq 0.75\pi$. Inset: excitonic $|00\rangle \rightarrow |10\rangle$ transitions in QD A and QD B coupled through V_{DD}. (b) Time dynamics of $\Delta R_{B,m}(\Delta t)$. The excitation conditions are the same as in (a) and the time resolution of the experiment is indicated (green solid line). (c) Rabi oscillation in a coupled QD. Magnitude of $\Delta R_{B,m}(\Delta t = 10$ ps$)$ as a function of the field amplitude of the pump laser. The solid line shows a simulation based on an optical Bloch equation model.

Now, optical nonlinearities are observed both at positive *and* negative Δt, the latter being evident from the non-instantaneous rise of the signal in Fig. 3(b). In contrast to the absorptive line shape in Fig. 2(b), the nonlinear spectra display a time-independent dispersive line shape, reflecting a transient *blueshift* of the exciton resonance which does not change much with time delay. From the amplitude and shape of the nonlinear spectra we deduce a line shift of $30 \pm 15 \mu$ eV around zero time delay. As seen in Fig. 3(b), the time evolution of $\Delta R_{B,m}$, defined as the difference between maximum and minimum of $\Delta R_B(\omega)$, is very different from that observed at the biexciton resonance. At negative time delays $\Delta R_{B,m}(\Delta t)$ shows a rise with a time constant of about 6 ps, followed by a slight dip and a slower decay on a time scale of more than 100 ps. The change of $\Delta R_{B,m}$ with the excitation field displays clear Rabi oscillations, in phase with those of Fig. 2(d).

To discuss these results, we stress the following observations. (i) Dispersive line shapes, caused by a transient blueshift of the QD resonance, are observed at all time delays and we find no signature of absorptive ΔR changes which would reflect pump-induced changes of the exciton population of QD *B*. This indicates that the observed nonlinearity is not due to an exciton relaxation between QD *A* and *B*. (ii) The presence of a strong laser field gives rise to transient excitonic line shifts via the optical Stark effect (OSE). However, as shown in [18], the OSE leads to optical nonlinearities at negative time delays ($\Delta t < 0$) only. Also, for a pump frequency above the exciton resonance, a redshift of the QD line is expected, in contradiction with our present findings. (iii) There is a clear correlation between the pulse-area dependence of ΔR_{XX} in Fig. 2(d) and of ΔR_B in Fig. 3(c).

The data in Fig. 3 thus reflect an electronic coupling between the QDs *A* and *B*. The most likely candidate for such an interaction is a dipole-dipole coupling between both QDs. Theoretical studies [5,6,19,20] indicate that two different mechanisms can contribute: resonant Förster energy transfer and direct Coulomb interaction between permanent excitonic dipole moments. For two quantum dots separated by less than the wavelength of light, pulsed optical excitation of one QD leads to the reemission of a transient electric field which can be reabsorbed by the second QD, thus (Förster) transferring the excitation. The interaction Hamiltonian $H_F = V_F p_A p_B^* +$ c.c. includes the coupling $V_F \propto \mu_A \mu_B / R_{AB}^3$ between coherent excitonic polarizations $p_i(t) = |10\rangle_i \langle 01|_i +$ c.c. in QDs *A* and *B*. The coupling strength is determined by the transition dipole moments $\mu_i = |\langle 00|\vec{M}_i|10\rangle_i|$ ($\vec{M}_i$: dipole operator) and the QD separation R_{AB}. In the strong coupling limit, $V_F/\hbar$ is larger than the detuning $\Delta\omega = \omega_A - \omega_B$ between the QD resonances and the dephasing rate $1/T_2$, leading to entangled states of the coupled system and cooperative effects in its radiative decay [8,20,21]. In the weak coupling limit, $V_F \ll \hbar\Delta\omega, \hbar/T_2$, the interaction induces a population relaxation between the coupled states [22].

The direct dipole interaction H_D, on the other hand, involves permanent excitonic dipole moments and thus interaction between the exciton populations $n_i = |10\rangle_i \times \langle 10|_i$ with $H_D = V_D n_A n_B$ and $V_D \propto d_A d_B / R_{AB}^3$. Here, d_i represents the permanent dipole moment originating from a shift of the electron and hole charge distributions in the exciton. This interaction leads to a biexcitonic energy shift V_D in case both QDs are excited [6].

To examine these two interaction mechanisms, nonlinear-optical spectra are calculated from the time evolution of the density matrix in rotating wave approximation. Here, the QDs are treated as effective two-level systems (states $|00\rangle_i$, $|10\rangle_i$), interacting with the pump and probe fields and coupled via the dipole-dipole interaction. Most of the parameters of these calculations such as ω_i, μ_i, $T_{2,i}$, and electric field profiles of the lasers are quantitatively known. The basic unknown is the mechanism and strength of the dipole-dipole interaction.

For the Förster mechanism, the time evolution of the spectra depends critically on the ratios of V_F, $\hbar\Delta\omega$, and $\hbar/T_2$. In our case, typical interdot distances are limited by the finite exciton size to about 20 nm, giving a coupling V_F of at most 30 μ eV for $\mu = 60$ D. Therefore, $V_F \lesssim \hbar/T_2$ (0.1 meV) $\ll \hbar\Delta\omega$ (3 meV); i.e., we are in the weak coupling limit. At negative delay times $\Delta t < 0$, $\Delta R_{B,m}$ is due to the optical Stark effect induced by the pump field with a dispersive line shape reflecting a redshift of the exciton line, and a rise of $\Delta R_{B,m}(\Delta t < 0)$ with $T_{2,B}$ [Fig. 4(a)]. At $\Delta t > 0$, the Förster mechanism induces exciton population relaxation between both QDs, resulting in absorptive line shapes. The decay of $\Delta R_{B,m}(\Delta t > 0)$ reflects both the exciton lifetime $T_{1,A} \simeq 40$ ps and the exciton transfer rate which scales as $\Gamma_F \propto V_F^2 T_2 [1 + (\Delta\omega T_2)^2]^{-1}$ [22]. Although the excitation field dependence of $\Delta R_{B,m}(\Delta t = 10$ ps) [Fig. 4(c)] displays Rabi oscillations, the line shapes and the temporal dynamics of $\Delta R_{B,m}$ are in disagreement with the experiment. Also, the amplitude of $\Delta R_{B,m}$ is much smaller than in the experiment. We infer that dipole coupling via the Förster mechanism is of minor importance for our QDs.

For a direct dipole interaction H_D between permanent excitonic dipole moments, excitation of QD *A* transiently shifts the energy of QD *B* by V_D. The sign of this shift depends on the sign of V_D and, thus, a blueshift occurs for parallel dipoles d_A and d_B. For a shift smaller than the homogeneous exciton linewidth, the coupling results in a dispersive shape of ΔR [Fig. 4(b)]. Both direct dipole coupling and OSE contribute to the line shifts at $\Delta t < 0$ and net blueshifts are observed if the Coulomb coupling is stronger than the OSE. The signal at $\Delta t < 0$ rises with $T_{2,B}$. For $\Delta t > 0$, $\Delta R_{B,m}$ decays exponentially with the exciton lifetime $T_{1,A}$, as there is no population transfer between the dots. The amplitude of $\Delta R_{B,m}$ monitors the exciton population in QD *A* and the intensity dependence of the pump-induced Rabi oscillation [Fig. 4(b)] is thus similar to that found in the single-exciton manipulation experiments.
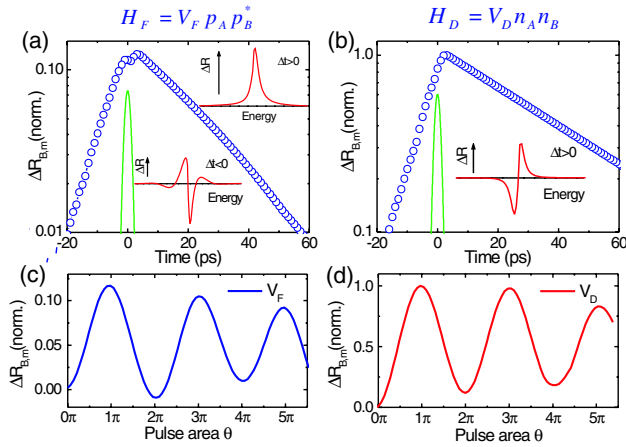
FIG. 4 (color online). (a) Simulation of optical nonlinearities of two QD coupled by Förster energy transfer for excitation conditions similar to Fig. 3. The nonlinear spectra (inset) display an absorptive line shape at $\Delta t > 0$ and dispersive redshifted line shape at $\Delta t < 0$. (b) Coupling via permanent excitonic dipole moments. For $V_D > 0$, the nonlinear spectra (inset) reflect a blueshift of the exciton line at all time delays. Pump-induced Rabi oscillations ($\Delta t = 10$ ps) for Förster (c) and for direct dipole coupling (d).

The experimental line shapes and Rabi oscillations are in good agreement with the direct coupling model. The calculated decay of $\Delta R_{B,m}$, however, is faster. This discrepancy may reflect signal contributions from more delocalized excitonic transitions in the environment of QD A [10]. Such states have smaller dipole moments and thus longer radiative lifetimes. Their presence may also lead to finite dipole shifts that persist on time scales longer than $T_{1,A}$. This notion is supported by finding experimentally a finite optical nonlinearity from QD B when the excitation pulse is slightly detuned from the resonance of QD A. For such a nonresonant excitation, however, Rabi oscillations are not observed. Apart from the permanent dipoles, the Coulomb interaction between excitons in QD A and B may lead to induced charge rearrangements which lower the energy (biexciton formation). The absence of a redshift in the experiment points to a dominance of dipole repulsion over such correlation effects.

It is interesting to ask whether the weak Förster coupling is a general property of this class of QD samples. The energy statistics of the localized exciton states are heavily influenced by level repulsion effects [10], resulting in finite energy splittings between excitons in neighboring QDs. Such splittings are typically 1–3 meV and thus stronger than the dipole coupling. Thus it is unlikely to find near-resonance situations between adjacent QDs and Förster coupling is most likely weak in general.

In conclusion, we have demonstrated the nonlinear-optical control of excitonic excitations in a pair of quantum dots coupled by dipole-dipole interaction. The coupling

strength of about 30 μ eV is still about 1 order of magnitude too small to implement a nonlocal conditional quantum gate as proposed in [6]. An increase in coupling should readily be achievable by applying moderate lateral electric fields, and two-qubit gating times of few ps seem feasible [19]. Recent progress in nanofabrication allows for manufacturing linear arrays of vertically and laterally stacked quantum dots with well-defined interdot distances. Such systems may permit us to go beyond two-qubit operations towards scalable qubit arrays, even though statistical variations of the coupling parameters within such arrays and excitation-induced decoherence pose technological challenges. Either energy-selective addressing (with inherently limited scalability) or cellular-automaton schemes [23,24] with globally applied multicolor pulse sequences may be used for encoding information in such arrays. The now established real-time probing of many-body interactions between individual solid-state nanostructures will be of key importance for future progress in this area.

*Electronic address: lienau@mbi-berlin.de
 [1] X. C. Hu and K. Schulten, Phys. Today **50**, No. 8, 28 (1997).
 [2] A. M. van Oijen et al., Science **285**, 400 (1999).
 [3] T.-Q. Nguyen et al., Science **288**, 652 (2000).
 [4] S. Woutersen and H. Bakker, Nature (London) **402**, 507 (1999).
 [5] L. Quiroga and N. F. Johnson, Phys. Rev. Lett. **83**, 2270 (1999).
 [6] E. Biolatti et al., Phys. Rev. Lett. **85**, 5647 (2000).
 [7] M. Ouyang and D. D. Awschalom, Science **301**, 1074 (2003).
 [8] C. Hettich et al., Science **298**, 385 (2002).
 [9] C. Hofmann et al., Phys. Rev. Lett. **90**, 013004 (2003).
[10] F. Intonti et al., Phys. Rev. Lett. **87**, 076801 (2001).
[11] D. Gammon et al., Phys. Rev. Lett. **76**, 3005 (1996).
[12] N. H. Bonadeo et al., Science **282**, 1473 (1998).
[13] D. P. DiVincenzo, Science **270**, 255 (1995).
[14] T. H. Stievater et al., Phys. Rev. Lett. **87**, 133603 (2001).
[15] T. Guenther et al., Phys. Rev. Lett. **89**, 057401 (2002).
[16] A. Zrenner et al., Nature (London) **418**, 612 (2002).
[17] X. Li et al., Science **301**, 809 (2003).
[18] T. Unold et al., Phys. Rev. Lett. **92**, 157401 (2004).
[19] E. Biolatti et al., Phys. Rev. B **65**, 075306 (2002).
[20] B. W. Lovett et al., Phys. Rev. B **68**, 205319 (2003).
[21] R. H. Dicke, Phys. Rev. **93**, 99 (1954).
[22] J. A. Leegwater, J. Phys. Chem. **100**, 14403 (1996).
[23] S. Lloyd, Science **261**, 1569 (1993).
[24] S. C. Benjamin, Phys. Rev. A **61**, 020301(R) (2000).